

Predicting Progression to Hypervascular HCC in Hypovascular Hypointense Nodules in Gadoteric Acid-enhanced MR Images in Patients with Chronic Liver Disease

Wanwarang Teerasamit, M.D., Suchanya Hongpinyo, M.D., Ranista Tongdee, M.D., Voraparee Suvannarerg, M.D.

Department of Radiology, Faculty of Medicine Siriraj Hospital, Mahidol University, Bangkok 10700, Thailand.

ABSTRACT

Objective: To identify patient characteristics and MR imaging features of hypovascular hypointense nodules in the hepatobiliary phase (HBP) of gadoteric acid-enhanced MR imaging in patients with chronic liver disease associated with progression to hypervascular hepatocellular carcinoma (HCC).

Materials and Methods: The institutional review board approved this retrospective review of 40 patients with 60 hypovascular hypointense nodules in the HBP of gadoteric acid-enhanced MR imaging. Univariate and multivariate Cox regression analyses for hypervascular HCC development were used to define variables, including initial nodule size, cause of cirrhosis, history of locoregional therapy of HCC, fat-containing, signal intensity on T1W, T2W, portal and equilibrium phases of dynamic phase, and DW images. The cumulative percentage incidence of hypervascularity and growth rate were calculated using the receiver operating characteristic (ROC) curve.

Results: The prevalence of progression to hypervascular HCC was 45% (27 out of 60). The Multivariable Cox analysis of developing hypervascularization was an initial nodule diameter more than 1 cm. ($P=0.027$; HR 2.52; 95% CI: 1.11,5.74) The mean growth rate was significantly higher in subsequent hypervascular nodules than in those without hypervascularization ($P < 0.001$). The cumulative risk incidence of hypervascularization at 3, 6, 12, 24 months was 5%, 20%, 35%, 44 %, respectively.

Conclusion: An initial nodule diameter of more than 1 cm and nodules with higher growth rates are significant predictive factors for hypervascular transformation of hypovascular hypointense nodules in the HBP of gadoteric acid-enhanced MR imaging.

Keywords: Gadoteric acid-enhanced MRI; hypovascular hypointense nodule in hepatobiliary phase; HCC imaging (Siriraj Med J 2023; 75: 680-687)

INTRODUCTION

Hepatocellular carcinoma (HCC) is one of the most common primary liver cancers in patients with chronic liver disease. The concept of multistep carcinogenesis in chronic liver disease or a cirrhotic liver involves regenerating nodules, dysplastic nodules and finally

HCC.¹⁻³ Surveillance via an ultrasound every six months is recommended for early detection.⁴⁻⁷ Further cross-sectional imaging, including multiphasic computed tomography (CT) or dynamic contrast-enhanced magnetic resonance imaging (MRI) of the liver should be performed for lesion characterization. Nowadays, HCC diagnosis is made

Corresponding author: Ranista Tongdee

E-mail: ranista@hotmail.com

Received 26 March 2023 Revised 7 August 2023 Accepted 7 August 2023

ORCID ID: <http://orcid.org/0000-0002-5879-3889>

<https://doi.org/10.33192/smj.v75i9.262021>



All material is licensed under terms of the Creative Commons Attribution 4.0 International (CC-BY-NC-ND 4.0) license unless otherwise stated.

through evidence of typical enhancement patterns that show arterial phase hyperenhancement with washout in portovenous and/or delayed phases, without any requirement of pathological confirmation.⁴⁻⁷ However, some small HCC does not show this typical enhancement pattern.⁸

Currently, gadoxetic acid disodium, a combined extracellular and hepatocyte-specific MR contrast agent is being increasingly used and improving the diagnostic accuracy of HCC.⁹ This agent has uptake in the normal hepatocyte in the hepatobiliary phase (HBP), and is seen with hypersignal intensity, whereas HCC cannot uptake it and results in hyposignal intensity.¹⁰ The feature of a hypointense nodule in HBP combined with hypervascularity in the arterial phase is indicative of HCC. Meanwhile, some hypointense nodules in HBP with no appearance of hypervascularity in the arterial phase are borderline nodules.^{11,12} These borderline nodules require close follow-up since they can convert into hypervascular HCC in follow-up imaging.¹³

The purpose of this study was to identify patient characteristics and MR imaging features of hypovascular hypointense nodules in HBP from gadoxetic acid-enhanced MRI in patients with chronic liver disease associated with progression to hypervascular HCC.

MATERIALS AND METHODS

Patients

This retrospective study was approved by our institutional review board (COA no. Si 507/2016). Our hospital picture archiving and communication system (PACS) database was searched for gadoxetic acid-enhanced MRI performed on patients with liver cirrhosis or chronic liver disease between 2012 to 2014.

The inclusion criteria included: patients with chronic liver disease aged above 18 who had hypovascular hypointense nodules in HBP from gadoxetic acid-enhanced MRI. These patients were required to undergo follow up either with gadoxetic acid-enhanced MRI, extracellular gadolinium-based MRI, or dynamic multiphase CT scans of the liver. Nodules which had characteristics of cyst, cystic tumor, hemangioma or hypovascular liver tumor such as cholangiocarcinoma or lymphoma were excluded from the study. Patients who had a history of transarterial chemoembolization (TACE) treatment before their initial MR imaging and last follow-up were not included. Any nodules with a history of post radiofrequency ablation (RFA) treatment were not included. However, patients who had a history of HCC with locoregional treatment such as surgery and RFA at other location were also included (Fig 1).

Baseline clinical data, cause of liver cirrhosis or chronic liver disease, Child-Pugh class and serum alpha-fetoprotein (AFP) level at the time of the initial MR image examination of each patients was also recorded.

MR examinations

The MR images were acquired using a whole body MR system Achieva 1.5-T; Philips Healthcare, Best, the Netherlands and two 3.0-T whole body MR systems (Ingenia 3.0-T and Achieva 3.0-T); Philips Healthcare, Best, the Netherlands.

The conventional MRI protocol consisted of axial T1-weighted dual fast field echo in-phase and opposed phase sequences, axial T2-weighted with fat suppression, axial T2 weighted turbo spin echo, and coronal single shot T2-weighted sequence. DWI was obtained before gadoxetic acid administration by using a respiratory-

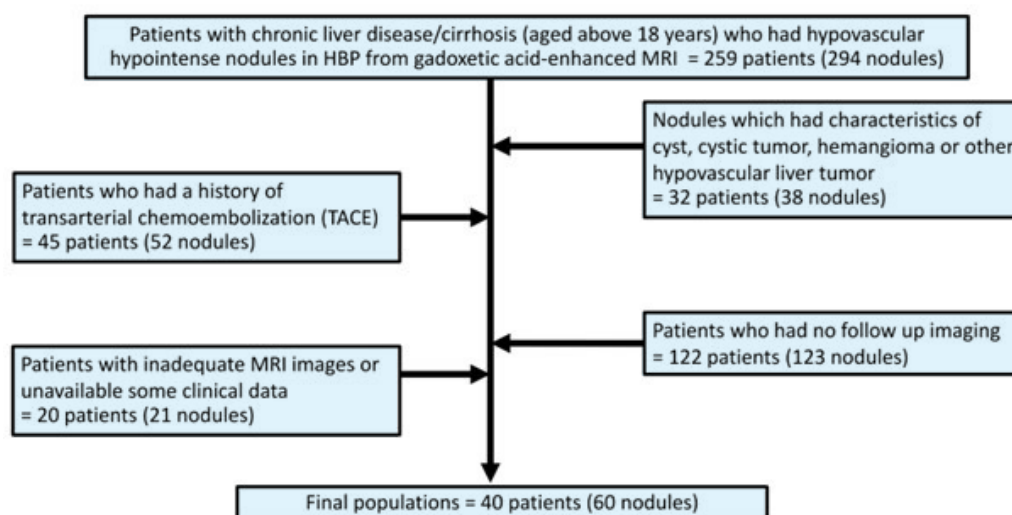


Fig 1. Final population of this study

triggered single-shot echo-planar imaging sequence with b values of 0, 50 or 150, 600 or 750 or 800 sec/mm². A spectral attenuated inversion-recovery technique was used for fat suppression on DWI. The apparent diffusion coefficient (ADC) map was generated by using b values of 0, 50 or 150, 600 or 750 or 800 sec/mm².

The MR contrast agent used was gadoxetic acid disodium (Primovist®; Bayer-Schering Healthcare, Berlin, Germany) which was administered at 0.1 mL/kg bodyweight (equivalent to 25 µmol/kg bodyweight). All injections were performed by a power injector at a rate of 1.5 mL/s through an antecubital vein and flushed with 30 mL saline administered at the same rate.

The dynamic study looked at suspended respiration at 30 seconds (arterial phase), 70 seconds (portovenous phase), 120 seconds and 5 minutes (transitional phase) after intravenous contrast administration. The hepatobiliary phase images were done at 20 and 30 minutes after contrast injection.

Image analysis

The initial MR images were evaluated with consensus by two abdominal radiologists; observer 1 (V.S., with 5 years of experience) and observer 2 (R.T., with 16 years of experience). Both were blinded to the clinical information, follow up MRI interpretations and the final diagnosis.

All lesions were preselected for review by a third abdominal radiologist (W.T., with 10 years of experience) who noted the image numbers, the segmental location of the lesion and marked them on the MR images.

All MR images were evaluated using PACS. Both observers were given the initial gadoxetic acid-enhanced MRI set (unenhanced T1 and T2-weighted images, gadoxetic acid-enhanced dynamic phase, hepatobiliary phase and DW images). The nodule size, presence of fat component, signal intensity on T1W, T2W, portal and transition phases of dynamic study, including hypersignal intensity in a high b-value DWI were investigated. The lesion sizes were measured as the longest diameter in hepatobiliary phase images. The presence of fat component was determined by decreased signal intensity of nodules on opposed phase T1W compared to in-phase T1W images. The signal intensity of the nodule surrounding the liver parenchyma was recorded relatively on T1W and T2W images and with high b values of DWI which can be described as hypointense, isointense and hyperintense. We evaluated the ADC for each nodule at the initial DWI. The b values of 0 and 600 or 800 sec/mm² were used to generate the ADC map.

The third radiologist was given the last follow up

image which could be either a gadoxetic acid-enhanced MR image, extracellular gadolinium-based enhanced MR image, or dynamic CT scan to define the transformation to hypervascular HCC. If the nodules showed signs of enhancement in the arterial phase, wash out on portal or transition phases with consistent hypointensity in the hepatobiliary phase, a diagnosis of “hypervascular HCC” was made.⁴⁻⁷ Meanwhile, nodules with no arterial enhancement and no progression in size were classified as “non-hypervascularization group”. The time between the initial to last images and the nodules’ sizes in the last follow up images were also recorded.

Statistical analysis

The clinical data was compared for hypervascular HCC and non-hypervascularization group. A two-sample t-test, Mann-Whitney U test were used to determine the difference in quantitative variables with (i.e., age, and duration of time between the first and the last imaging) and without normal distribution (serum AFP) between the HCC and non-HCC group. A Pearson’s chi-square test was used to compare qualitative variables between the two groups.

The time to HCC development was calculated from the date of initial MR imaging to the final follow-up. A Kaplan-Meier survival curve was constructed for qualitative variables (e.g., T2W image and DW image). The univariate Cox regression analysis was used to determine the effect of each factor towards the time of HCC development. A forward multivariate Cox regression analysis was performed to identify predictive variables for HCC after adjusting for other characteristics. The adjusted hazard ratio and 95% confidence intervals (CIs) were also calculated.

The growth rate was computed as the difference between the initial and final diameter of nodules (millimeters), divided by duration (days) in initial and final MR imaging. The difference in growth rate between the two groups was compared using a Mann-Whitney U test. The prognostic value of the growth rate was evaluated using the receiver operating characteristic (ROC) curve.

All tests were two sided, and a p-value of less than 0.05 was considered statistically different. All statistical analyses were performed using PASW version 18.

RESULTS

Baseline clinical data was collected from a total of 40 patients (30 men and 10 women). The age range of male patients was 42-81, with a mean age of 60.9; while the range of female patients was 50-81, with a mean age of 64.09.

The cause of liver cirrhosis or chronic liver disease was also obtained and the results were as follows: chronic hepatitis B viral infection (n=25), chronic hepatitis C viral infection (n=8), alcoholic cirrhosis (n=3), non-alcoholic steatohepatitis (NASH) (n=2), hemochromatosis (n=1), and cryptogenic cirrhosis (n=1). Almost all patients were classified in Child-Pugh class A except one who was classified as Child-Pugh class C. The serum alpha-fetoprotein (AFP) level at the time of the initial MR image examination was also recorded.

A total of 60 hypovascular hypointense nodules in HBP of gadoxetic acid-enhanced MRI were identified in 40 patients; 28 had a single nodule, seven had two nodules, three had three nodules, one had four nodules, and 1 other had five nodules. Of these, 27 nodules showed progression to hypervascular HCC upon follow-up imaging (Group 1) while 33 nodules did not change to hypervascular HCC in a follow-up MRI (Group 2). All Group 1 nodules were underwent the specific treatment of HCC, including TACE (14/27 nodules = 51.85%, RFA 12/27 nodules = 44.45%, surgery 1/27 nodule = 3.7%). All patients in Group 2 underwent a follow-up MRI and there was no evidence of hypervascular HCC.

A mean follow-up time of 674.63 ± 407.87 days (range 62-1341 days), hypervascular HCC was seen in 27 out of 60 nodules (45%) while 33 out of 60 nodules (55%) did not show progression to hypervascular HCC. All nodules were diagnosed on the basis of gadoxetic acid-enhanced MRI. The cumulative incidence of hypervascular transformation at 3, 6, 12 and 24 months was as follows: 5%, 20%, 35%, and 44%, respectively (Fig 2). Hypovascular hypointense nodules in HBP combined with hyperintensity in T2W

images had median time to hypervascular HCC of 118 days. Hypovascular hypointense nodules in HBP combined with hyperintensity DW images had a median time to hypervascular HCC of 137 days and was statistically significant ($P < 0.001$).

The baseline clinical data between two groups, including age, sex and serum AFP of patients show no statistically significant difference between the two groups.

MR imaging features of both groups are summarized in Table 1. A Univariate Cox regression analysis (Table 1) revealed that hyperintensity on T2W images, hypersignal intensity on DWI, and history of previous HCC were statistically significant and associated with progression to hypervascular HCC. These variables were entered into the multivariate Cox analysis, which included the initial size of the nodules (Table 2). Only initial sizes of nodules greater than 1 centimeter were statistically significant and associated with progression to hypervascular HCC (Adjusted HR 2.52; 95% CI: 1.11, 5.74) (Fig 3).

Hyperintensity on T2W images seemed to increase the risk of progression to hypervascular HCC but this was not statistically significant ($P = 0.308$; Adjusted HR 4.77; 95%CI: 0.24, 95.95). Hyperintensity on DW images also tended to increase the risk of hypervascular HCC but this was also not statistically significant ($P = 0.597$; Adjusted HR 1.93; 95%CI: 0.17, 22.22). However, most hypervascular HCC groups (19 out of 27 nodules, 70.4%) did not show hyperintensity on T2W images and/or hyperintensity on DW images in initial MR imaging. The history of locoregional treatment for HCC is associated with progression to hypervascular HCC ($P = 0.059$; adjusted HR 2.27; 95%CI: 0.97, 5.34).

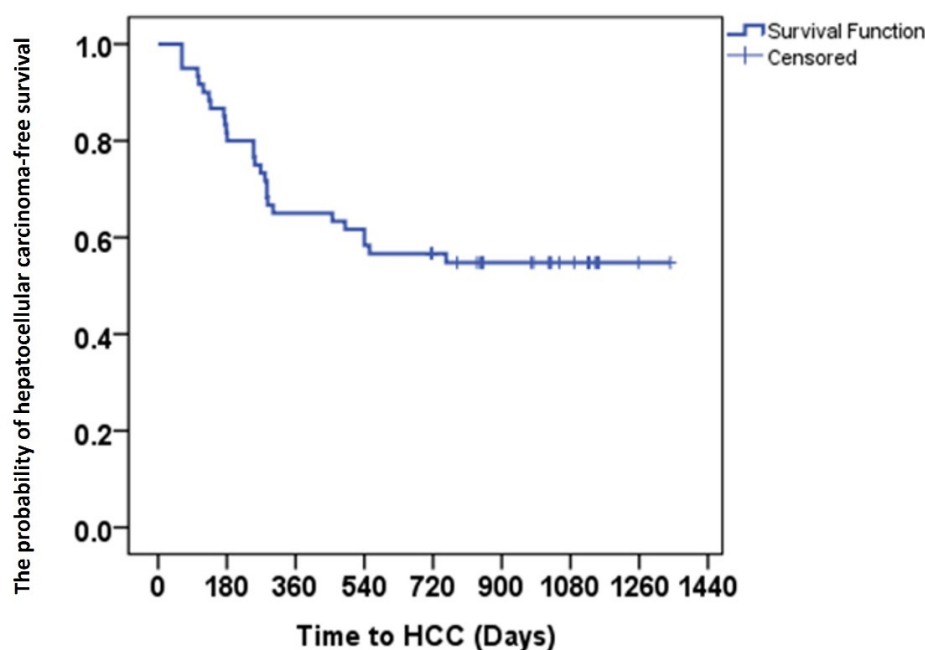


Fig 2. The probability of hepatocellular carcinoma-free survival for all hypovascular hypointense nodules in the hepatobiliary phase.

TABLE 1. Characteristics and Univariate Cox analysis for developing hypervascular HCC

Parameter	Number of patients (%)		Univariate Cox Model	
	HCC	Non-Hypervascularization	HR (95%CI)	P-value
Fat containing				
Yes	6 (46.2)	7 (53.8)	0.96 (0.39,2.37)	0.956
No	21 (48.8)	22 (51.2)	1.00	
T1W				
Hyperintensity	4 (40.0)	6 (60)	0.703(0.2,2.5)	0.586
Isointensity	17 (45.9)	20 (54.1)	0.75 (0.3,1.91)	0.545
Hypointensity	6 (46.2)	7 (53.6)	1.00	
T2W				
Hyperintensity	8 (88.9)	1 (11.8)	16.03(1.98,129.88)	0.009
Isointensity	18 (40.9)	26 (59.1)	2.99 (0.40,22.40)	0.287
Hypointensity	1 (14.3)	6 (85.1)	1.00	
Portal				
Isointensity	11 (44.0)	14 (56)	1.00	
Hypointensity	16 (45.7)	19 (54.1)	1.11(0.52,2.4)	0.789
Equilibrium				
Isointensity	3 (37.5)	5 (62.3)	1.00	
Hypointensity	24 (46.2)	28 (53.2)	1.36 (0.41,4.53)	0.612
DW image				
Hyperintensity	8 (88.9)	1 (11.8)	5.75 (2.46,13.44)	<0.001
Isointensity	19 (37.8)	32 (62.1)	1.00	
History of local therapy for HCC				
Yes	16 (61.5)	10 (38.1)	2.44(1.13,5.27)	0.023
No	11 (32.4)	23 (67.1)	1.00	
Initial diameter				
>1 cm	12 (60.0)	8 (40)	2.01 (0.94,4.31)	0.071
≤ 1 cm	15 (37.5)	25 (62.1)	1.00	
Cirrhosis				
HBV	17 (54.8)	14 (45.1)	1.21 (0.47,3.07)	0.694
HCV	4 (25)	12 (75)	0.42(0.12,1.47)	0.173
Non HBV/HCV	6 (46.2)	7 (53.6)	1.00	

TABLE 2. Multivariate analysis by Cox regression model for hypovascular hypointense nodules in HBP using gadoxetic acid-enhanced MRI to transform into hypervascular HCC

Characteristics	P-value	Adjusted HR	95%CI
T2W			
Hyperintense	0.308	4.77	(0.24,95.95)
Isointense	0.549	1.89	(0.24,15.03)
Restricted Diffusion	0.597	1.93	(0.17,22.22)
History of local therapy for HCC	0.059	2.27	(0.97,5.34)
Size > 1 cm	0.027	2.52	(1.11,5.74)

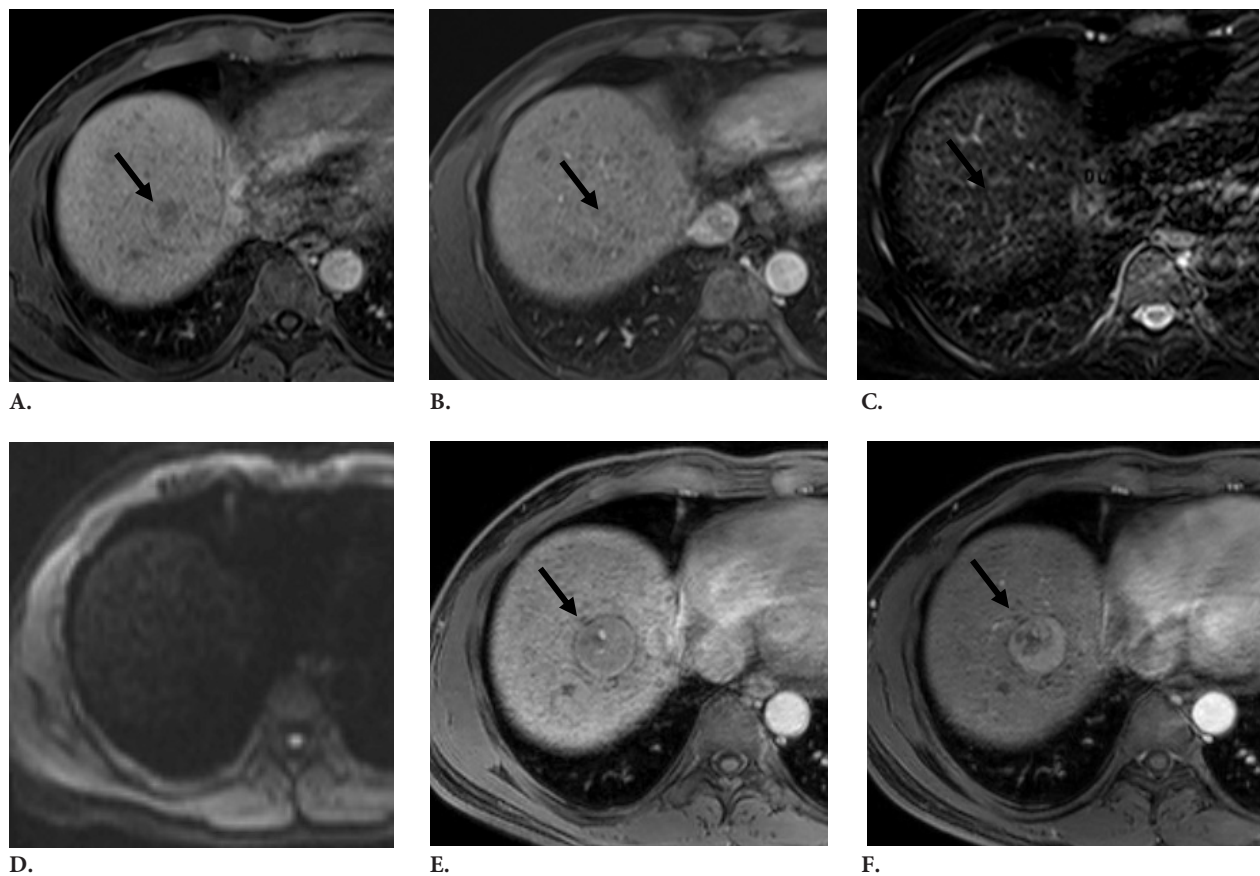


Fig 3. A 53-year-old male with HCV cirrhosis. (A) Axial gadoxetic acid-enhanced 20 minute HBP image showing a hypointense nodule, initial diameter of about 1.7 cm. (B) Axial arterial phase showing no arterial enhancing nodule at the same location. (C) Axial T2W image and (D) DW image ($b = 800 \text{ sec/mm}^2$) observed no hypersignal intensity. (E,F) Axial gadoxetic acid-enhanced MRI obtained later 9 months, the same nodule showed increased in diameter to 3.1 cm. measured in (E) hepatobiliary phase image. (F) Arterial phase showing hypervascularization.

Growth analysis of the two groups was also recorded. Twenty-seven nodules in the hypervascular HCC group (initial diameter $10.4 \text{ mm} \pm 4.5$) (range, 5-21 mm) and thirty-three nodules in the non-hypervascularization group (initial diameter $8.2 \text{ mm} \pm 3.5$) (range, 4-16 mm) were evaluated. The median time of observation was 269.7 ± 178.21 days (range 62-754) in the hypervascular HCC group and 1005.94 ± 171.37 days (range 716-1341) in the non-hypervascularization group.

In the hypervascular HCC group, 26 nodules increased in size and one nodule remained stable during follow-up imaging. The median growth rate in the hypervascular HCC group was $19.4 \times 10^{-3}/\text{day}$. In the non-hypervascularization group, the median growth rate was $-0.8 \times 10^{-3}/\text{day}$. By using the Mann-Whitney U test, the mean growth rate of hypervascular HCC group was higher than the non-hypervascularization group ($p < 0.001$). The ROC analysis (area under the curve, 0.985) had a growth rate cutoff value of 3.1×10^{-3} per day, sensitivity of 92.59% and specificity of 96.97%, positive predictive value (PPV) of 96.15% (25 of 26 nodules) and negative predictive value (NPV) of 94.12% (32 out of 34 nodules).

DISCUSSION

Due to the multistep hepatocarcinogenesis concept, the hypovascular hypointense nodule in HBP can progress to hypervascular HCC in serial follow-up MR imaging.¹⁴⁻¹⁶ This recent study showed that the cumulative percentage incidence of hypervascular transformation at 6 months, 1 and 2 years were 20%, 35%, and 44%, respectively. These results are apparently more than the cumulative incidence rates from a meta-analysis¹⁶ which found a pooled 1 and 2-year cumulative incidence rate of 18.3% and 25.2%, respectively. This difference is reflected in the high prevalence of HCC in our region, which requires strict interval follow-up of these nodules.

This study found that a initial nodule size (more than 1 centimeter) is the only significant predictive factor for hypervascular transformation of hypovascular hypointense nodules in HBP, similar to the previous report.¹⁵⁻¹⁷ Moreover, the mean growth rate of nodules that progress to hypervascular HCC was significantly higher than the non-hypervascularization group. According to the receiver operating characteristic (ROC) curve, a cut-off growth rate of 3.1×10^{-3} per day in this study is higher

than a previous report.¹⁸ Nodules with a growth rate of more than 3.1×10^{-3} per day are related to subsequent hypervascular HCC. The authors suggest that hypovascular hypointense nodules in HBP larger than 1 cm in diameter with a fast growth rate be closely follow up.

Nevertheless, the Univariate Cox analysis from this study revealed hypersignal intensity on T2W and DW images and a history of local therapy for HCC associated with progression to hypervascular HCC. These results are in accordance with previous studies.¹⁷⁻²¹ Kim YK *et al.*²⁰ reported that hypersignal intensity on DW images strongly associated with progression to hypervascular HCC. Hyodo *et al.*¹⁸ also noted that hyperintensity on T2W images was a strong risk factor for subsequent hypervascularization. Although these MRI features and patient characteristics were not statistically significant when using a Multivariate Cox regression analysis in this study, it tended to increase the risk of development of hypervascular HCC. The authors also suggest that hypovascular hypointense nodules with these suspicious imaging features or a history of local therapy for HCC with higher growth rates should be closely followed-up for the development of hypervascular HCC in the future.

This study had several limitations. First, the number of patients included in this single-center study was small. Second, this was a retrospective study, and therefore there may have been selection bias. Third, our MR imaging protocols had various b-values for DW imaging which may have had an effect on interpretation of signal intensity of the nodules. Fourth, there was no pathological result correlation, and thus the ability to identify the exact stage of these nodules in multistep carcinogenesis was not available.

In conclusion, hypovascular hypointense nodules in the HPB of gadoxetic acid-enhanced MRI can potentially progress to hypervascular HCC in the future. A initial nodule diameter of more than 1 cm and nodules with higher growth rate are significant predictive factors for hypervascular transformation.

REFERENCES

1. Sakamoto M, Hirohashi S, Shimosato Y. Early stages of multistep hepatocarcinogenesis: adenomatous hyperplasia and early hepatocellular carcinoma. *Hum Pathol.* 1991;22(2):172-8.
2. Takayama T, Makuuchi M, Hirohashi S, Sakamoto M, Okazaki N, Takayasu K, et al. Malignant transformation of adenomatous hyperplasia to hepatocellular carcinoma. *Lancet.* 1990;336(8724):1150-3.
3. Kudo M. Multistep human hepatocarcinogenesis: correlation of imaging with pathology. *J Gastroenterol.* 2009;44(Suppl 19):112-8.
4. Marrero JA, Kulik LM, Sirlin CB, Zhu AX, Finn RS, Abecassis MM, et al. Diagnosis, staging, and management of hepatocellular carcinoma: 2018 practice guidance by the american association for the study of liver diseases. *Hepatology.* 2018;68(2):723-50.
5. EASL Clinical Practice Guidelines: Management of hepatocellular carcinoma. *J Hepatol.* 2018;69:182-236.
6. 2018 Korean Liver Cancer Association-National Cancer Center Korea Practice Guidelines for the management of hepatocellular carcinoma. *Korean J Radiol.* 2019;20(7):1042-113.
7. Omata M, Cheng AL, Kokudo N, Kudo M, Lee JM, Jia J, et al. Asia-Pacific clinical practice guidelines on the management of hepatocellular carcinoma: a 2017 update. *Hepatol Int.* 2017;11:317-70.
8. Yoon SH, Lee JM, So YH, Hong SH, Kim SJ, Han JK, et al. Multiphasic MDCT enhancement pattern of hepatocellular carcinoma smaller than 3 cm in diameter: tumor size and cellular differentiation. *AJR.* 2009;193:482-9.
9. Teerasamit W, Tongdee R, Yodying J. Diagnostic Performance of Gadoteric Acid-Enhanced MR Imaging in the Diagnosis of Hepatocellular Carcinoma in Cirrhotic Liver. *J Med Assoc Thai.* 2017;100(8):918-26.
10. Cruite I, Schroeder M, Merkle EM, Sirlin CB. Gadoteric acid-enhanced MRI of the liver: part 2, protocol optimization and lesion appearance in the cirrhotic liver. *AJR Am J Roentgenol.* 2010; 195:29-41.
11. Kim MJ. Current limitations and potential breakthroughs for the early diagnosis of hepatocellular carcinoma. *Gut Liver.* 2011; 5(1):15-21.
12. Park HJ, Choi BI, Lee ES, Park SB, Lee JB. How to differentiate borderline hepatic nodules in hepatocarcinogenesis: Emphasis on imaging diagnosis. *Liver Cancer.* 2017;6:189-203.
13. Hayashi M, Matsui O, Ueda K, Kawamori Y, Gabata T, Kadoya M. Progression to hypervascular hepatocellular carcinoma: correlation with intranodular blood supply evaluated with CT during intraarterial injection of contrast material. *Radiology.* 2002;225(1):143-9.
14. Kumada T, Toyoda H, Tada T, Sone Y, Fujimori M, Ogawa S, et al. Evolution of hypointense hepatocellular nodules observed only in the hepatobiliary phase of gadoteric acid-enhanced MRI. *Am J Roentgenol.* 2011;197:58-63.
15. Motosugi U, Ichikawa T, Sano K, Sou H, Onohara K, Muhi A, et al. Outcome of hypovascular hepatic nodules revealing no gadoteric acid uptake in patients with chronic liver disease. *J Magn Reson Imaging.* 2011;34:88-94.
16. Suh CH, Kim KW, Pyo J, Lee J, Kim SY, Park SH. Hypervascular transformation of hypovascular hypointense nodules in the hepatobiliary phase of gadoteric acid-enhanced MRI: a systematic review and meta-analysis. *AJR Am J Roentgenol.* 2017; 209(4): 781-9.
17. Kim YS, Song JS, Lee HK, Han YM. Hypovascular hypointense nodules on hepatobiliary phase without T2 hyperintensity on gadoteric acid-enhanced MR images in patients with chronic liver disease: long-term outcomes and risk factors for hypervascular transformation. *Eur Radiol.* 2016; 26(10):3728-36.
18. Hyodo T, Murakami T, Imai Y, Okada M, Hori M, Kagawa Y, et al. Hypovascular nodules in patients with chronic liver disease: risk factors for development of hypervascular hepatocellular carcinoma. *Radiology.* 2013;266(2):480-90.
19. Lee MH, Kim SH, Park MJ, Park CK, Rhim H. Gadoteric acid-enhanced hepatobiliary phase MRI and high b-value diffusion weighted imaging to distinguish well-differentiated hepatocellular carcinomas from benign nodules in patients with chronic liver

- disease. *AJR Am J Roentgenol*. 2011;197:W868-W75.
20. Kim YK, Lee WJ, Park MJ, Kim SH, Rhim H, Choi D. Hypovascular hypointense nodules on hepatobiliary phase gadoxetic acid – enhanced MR images in patients with cirrhosis: Potential of DW imaging in predicting progression to hypervascular HCC. *Radiology*. 2012;266(2):104-12.
21. Briani C, Pietropaolo MD, Marignani M, Carbonetti F, Begini P, David V, et al. Non-Hypervascular Hypointense Nodules at Gadoteric Acid MRI: Hepatocellular Carcinoma Risk Assessment with Emphasis on the Role of Diffusion-Weighted Imaging. *J Gastrointest Cancer*. 2018; 49(3):302-10.